Investigating the interaction between melamine and cyanuric acid using a Physiologically-Based Toxicokinetic model in rainbow trout

Cléo Tebby, Céline Brochot, Jean-Lou Dorne, Rémy Beaudouin

Investigating the interaction between melamine and cyanuric acid using a Physiologically-Based Toxicokinetic model in rainbow trout

Cleo Tebby[a], Céline Brochot[a], Jean-Lou Dorne[b], Rémy Beaudouin[a,c,1]

[a] Institut National de l'Environnement Industriel et des Risques (INERIS), Models for Ecotoxicology and Toxicology Unit, Parc ALATA, BP2, 60550 Verneuil-en-Halatte, France

[b] European Food Safety Authority (EFSA), Scientific Committee and Emerging Risks Unit, Via Carlo Magno 1A, 43126 Parma, Italy

[c] Institut National de l'Environnement Industriel et des Risques (INERIS), UMR-I 02 SEBIO, Parc ALATA, BP2, 60550 Verneuil-en-Halatte, France

[1] Corresponding author: Rémy Beaudouin

Institut National de l'Environnement Industriel et des Risques (INERIS), Models for Ecotoxicology and Toxicology Unit, Parc ALATA, BP2, 60550 Verneuil-en-Halatte, France

Tel: +33 3 44 61 82 38

Email: remy.beaudouin@ineris.fr

Abstract

Following outbreaks of feed and food adulterations with a melamine and cyanuric acid mixture in 2007 and melamine in 2008 respectively, the kinetics and toxicodynamics of the mixture have been investigated particularly in sensitive species such as the rainbow trout. Tissue concentrations and intensity of the adverse effect, melamine-cyanurate crystal formation in kidney, were reported in similar experimental conditions. Here, a recent PBTK model for rainbow trout has been applied to model the kinetics of both single compounds based on residue levels in tissues. Both PBTK models for the single compounds were combined and a model of crystal formation for the mixture melamine-cyanuric acid was also added to predict the intensity of crystal formation under the assumptions that crystals formed either in urine or in kidney tissue. Modelling the kinetics of melamine and cyanuric acid provided a better understanding and prediction of intensity of crystal formation in case of sequential exposures with varying intensity or co-exposure.

This study demonstrates, for the first time, how fish PBTK models can play a key role in the understanding and prediction of toxicokinetics and toxicodynamics of mixtures. This study also illustrates how adverse effects may potentially occur even when the compounds are not administered together as a mixture.

Keywords: Physiologically-Based Toxicokinetic (PBTK) model; toxicodynamics; mixture; interaction; melamine; rainbow trout

Introduction

After the outbreak of melamine (MEL) poisoning in infants related to food adulteration in 2008 (Baynes and Riviere, 2010), concern arose over MEL residue levels in farmed domestic animals (Gossner et al., 2009). Indeed, at the same period, mass death in cats and dogs in the USA was attributed to a large scale pet food adulteration with MEL and one of its analogs, cyanuric acid (CYA) (Baynes and Riviere, 2010; Brown et al., 2007; Puschner et al., 2007). The cause of renal failure in infants and in domestic animals was attributed to a reaction of MEL either with uric acid (Skinner et al., 2010), which is a normal component of urine, or with CYA, in the case of co-exposure. In 2009, EFSA derived a tolerable daily intake (TDI) for MEL and its analogues in food of 0.19 mg/kg body weight per day by applying a default uncertainty factor of 100 (Dorne et al., 2013). At this time, very few single dose studies were available on the toxicity of the mixture of MEL and CYA with no dose response data to assess the magnitude of the synergistic effects. Both toxicity and kinetics of MEL were consequently studied in swine (Buur et al., 2008; Wang et al., 2014; Xing et al., 2014), poultry (Brand et al., 2012; Zapletal et al., 2016) and fish (Phromkunthong et al., 2015; Pirarat et al., 2012) which were intended for human consumption. The kinetics and effects of MEL combined with CYA were studied in particular in rainbow trout (*Oncorhynchus mykiss*) (Liu et al., 2014; Pacini et al., 2014; Pacini et al., 2013; Reimschuessel et al., 2009a; Reimschuessel et al., 2010; Reimschuessel et al., 2008; Stine et al., 2013; Stine et al., 2012), one of the most farmed fishes worldwide (FAO, 2017).

MEL is a highly polar basic compound. CYA is a structural analogue of MEL and is a weak acid. It is also a metabolite of MEL (Jutzi et al., 1982), and although most MEL is excreted without being metabolized by mammals, it has been suggested that gut bacteria can metabolize MEL into CYA (Brand et al., 2012; Seffernick et al., 2010; Wackett et al., 2002; Zapletal et al., 2016), thus resulting in combined toxicity. When combined, MEL and CYA act synergistically due to crystal formation (Puschner et al., 2007). The neutral forms of MEL and CYA form high molecular weight complexes of melamine cyanurate (MEL-CYA) with equal molar amounts of both compounds, linked by hydrogen bonds and aromatic ring stacking (Seto and Whitesides, 1990), sometimes referred to as a "salt". Formation of MEL-CYA is therefore pH-dependent. MEL-CYA precipitates to form crystals,

that can be needle-like precipitates, spherulites, or tubular-shaped depending on the environment in which they form (Reimschuessel et al., 2010; Tolleson, 2010). MEL-CYA complex (CASRN: 37640-57-6) is used as a flame retardant (Casu et al., 1997) and has low, pH-dependent, solubility (around 1 to 10 mg/L at 20°C) and low bioavailability (Jacob et al., 2012; Reimschuessel et al., 2008) compared to MEL and CYA (solubilities of 3240 mg/L at 20°C and 2000 mg/L at 25°C respectively according to the Human Metabolome Database).

Studies of the kinetics of MEL alone or in combination with CYA have revealed small changes in kinetics of MEL in the case of co-exposure in some studies, with delayed disposition of MEL (Xue et al., 2011), delayed disposition of MEL and CYA (Reimschuessel et al., 2009a) or lower absorption and excretion and increased tissue accumulation of MEL in rats (Pang et al., 2013) although in other studies no significant alteration was observed (Jacob et al., 2012). It is unclear to which extent the observed kinetic interaction is related to a decrease in the amount absorbed through the gut due to decreased bioavailability as suggested by Pang et al. (2013) and Reimschuessel et al. (2008) or to crystal formation inside the organism leading to sequestration within tissues (Pang et al., 2013) or in the urinary tract. By modelling the kinetics of the single compound kinetics, kinetics of the mixture can be predicted under various assumptions on the type of interaction between the compounds.

Physiologically-based toxicokinetic (PBTK) models are used to describe the kinetics of xenobiotics in the organism by modelling absorption, distribution, metabolism, and excretion (Gerlowski and Jain, 1983). PBTK models have been developed for a wide range of organisms, including fish (Grech et al., 2017), and in particular for rainbow trout (Grech et al., 2019; Nichols et al., 1990).

In this paper, we extend the PBTK model for rainbow trout developed by Grech et al. (2019), to predict kinetics of MEL and CYA in the whole fish, with a focus on the kidney for the prediction of crystal formation. This model was originally applied to single compounds. In this paper, it was therefore extended to predict concentrations of both MEL and CYA simultaneously. Specific equations were also integrated in the model to quantify the physical interaction between MEL and CYA.

In this paper, the kinetics of both MEL and CYA administered orally either in separate experiments or as binary mixtures or sequentially to rainbow trout (toxicokinetic part) and intensity of crystal formation (toxicodynamic part) were modelled to investigate their interaction mechanisms. To this purpose, the kinetics of MEL and CYA and the intensity of crystal formation were predicted according to two interaction scenarios which depict two very different situations. Scenario (1) models crystal formation in urine, which does not result in any toxicokinetic interaction, and scenario (2) models crystal formation in the kidney which influences the toxicokinetics of the single compounds. The aim is to provide indication of the range of outcomes that can be predicted without modelling the complexity of the renal structure and the urine formation process, and which provides best predictions of the adverse effect.

Material and methods

Data

Toxicokinetic data on single compounds and mixtures

Data on single compounds kinetics were collected from the literature in four different studies (Liu et al., 2014; Pacini et al., 2013; Reimschuessel et al., 2009a; Stine et al., 2013; Stine et al., 2012; Xue et al., 2011) (Table 1). The compounds were orally administered as single or repeated doses, either mixed into feed or in capsules administered by gavage. The fish mean bodyweight at the start of the experiment ranged from 107g to 408g. The temperature ranged from 10 to 16°C. MEL or CYA were dosed at multiple or single timepoints in muscle, serum or plasma, kidney, or liver.

Toxicodynamic data on melamine cyanurate crystal formation

Two studies have quantified renal crystal formation after combined or sequential administration of MEL and CYA (Table 2, and Table 1 in SI). These studies are closely related to the toxicokinetic studies A1 and F (Table 1) since they were performed in the same facilities (A1 and A2) and with the same group of fish (F). Reimschuessel et al. (2010) quantified crystal formation after 1, 4, 14, or 28 daily doses of MEL and CYA in combination, and after sequential exposures to MEL and CYA with

several waiting periods between doses. Renal crystal formation was also studied by Pacini et al. (2014) in a 10-week experiment with daily doses of MEL and CYA administered together.

In both studies, kidney sections were examined using "wet-mount" microscopy. Crystals were measured and enumerated using the same methodology in both studies: crystal intensity was graded on a 0-4 scale where 0 indicated there were no crystals and 4 indicated an extensive number of crystals.

PBTK model for single compounds

Description of the PBTK model

The PBTK model for rainbow trout developed by Grech et al. (2019) (Figure 1) extends PBPK models developed previously for fish (Nichols et al., 1990; Pery et al., 2014). This PBPK model includes twelve well-mixed compartments, with blood-flow limited distribution of compounds. Cardiac output, oxygen consumption rate, and afferent oxygen concentration are modulated by temperature by using Arrhenius' function. The model also integrates a growth model based on the DEB theory (Kooijman, 2010) in which the parameters depend on the temperature and the food level as in Beaudouin et al. (2012). In its generic version, the model includes branchial and intestinal absorption routes and branchial, urinary, fecal, and biliary excretion routes. The rainbow trout model was parameterized based on a meta-analysis of literature data that was specific to this species. In this paper, we added the effect of temperature on the first-order rates of oral absorption and urinary excretion, using the Arrhenius equation as done by Grech et al. (2019) for other physiological processes. Temperature can affect urinary excretion directly or by modulating cardiac output (and, as a consequence, the blood flow to the kidney), and /or the absorption rate and ultimately affects internal concentrations. In addition to the sensitivity analysis performed by Grech et al. (2019) on the whole PB-TK model, a sensitivity analysis has been performed here using a slightly modified model to determine the processes under which temperature may affect urinary excretion (see section 4 in SI).

The food level parameter in the DEB model was adjusted according to the growth reported over the 8-week experiment by Pacini et al. (2013) and set to 0.3 in all simulations, based on the 1% reported feeding rate. The trout were assumed to urinate 1.2 $mL.kg^{-1}$ every 30 minutes (Curtis and Wood,

1991). In our model, we assumed a residual bladder volume of 1 % with no difference in release of single compounds or MEL-CYA complex.

Calibration of chemical-specific parameters

MEL and CYA are structural analogues, therefore the PBTK model parameterization was similar for both compounds. The parameterization relies on several assumptions. First, fecal excretion was assumed to be negligible as reported for MEL in swine (Buur et al., 2008) and rats (Mast et al., 1983) and for low doses of CYA in rats (Reimschuessel et al., 2009b). Secondly, in fish, organic compounds are excreted by various routes depending on their molecular weight, polarity, and lipophilicity. Compounds can be excreted by gills, in particular compounds with low to moderate lipid solubility (log K_{ow} between 1 and 4) (Nagel and Urich, 1980; Thomas and Rice, 1982), in bile, in particular large (over 600 g/mol) polar compounds (Gingerich et al., 1977; Schmidt and Weber, 1973), or by a minor route, urine, in particular for small polar compounds, with a large unbound fraction in plasma (Miller, 1987; Pritchard and Renfro, 1984), or some highly bound chemicals such as perfluorooctanoic acid (PFOA) (Consoer et al., 2014). MEL and CYA being relatively small polar compounds, urinary excretion may be an important route. Gill excretion is unlikely to play a major role since the logKow of MEL and CYA are -1.37 and -0.47 respectively but it may occur if the chemicals are in an ionized form. This has been demonstrated in a study highlighting that such ionized forms were more bioavailable for uptake through the gills compared with neutral forms (Erickson et al., 2006). MEL may therefore be poorly bioavailable at pH 7, and therefore not readily absorbed or excreted. On the other hand, CYA has a higher pKa and is approximately half ionized at pH 7, so branchial excretion cannot be totally excluded. As no data was available on the ratio of urinary vs. branchial excretion of absorbed MEL or CYA, excretion was assumed to be exclusively urinary.

The generic PBTK model included QSAR models for partition coefficients but they were designed for hydrophobic compounds (Bertelsen et al., 1998; Nichols et al., 2006; Pery et al., 2014). Both MEL and CYA were outside the domain of applicability of the QSAR models as their logKow were negative.

The partition coefficients, intestinal absorption rates, and excretion rates were calibrated using Bayesian methods (methods and code detailed in sections 2 and 5 in SI). For both compounds, the

intestinal absorption and excretion rates were calibrated together with the kidney to blood partition coefficient, and one partition coefficient for all other tissues with the exception of the liver. For MEL, the liver to blood partition coefficient was estimated and for CYA, it was set to the estimate obtained with MEL because no data was available for CYA in the liver. The prior distributions for the partition coefficients were based on the values used in a PBPK model for MEL in swine (Buur et al., 2008) and are detailed in Section 2 in SI.

Interaction model

Crystal formation model

The interaction between MEL and CYA was modelled as a stoichiometric reaction between the neutral forms of MEL and CYA as a pH-dependent reaction so that both compounds must be present at the same time and the compound with the lowest concentration limits MEL-CYA formation. Modelling this interaction required adding equations in the generic rainbow trout PBTK model to describe the equilibrium between neutral and ionized forms of MEL and CYA as well as MEL-CYA complex formation and precipitation. The neutral fractions of MEL and CYA were calculated assuming that the ionized/neutral equilibrium is instantaneous with the Henderson-Hasselbalch equation (Eq. 1).

$$f_{neutral} = \frac{1}{1+10^{\alpha(pH-pKa)}} \quad \text{Eq. 1}$$

Where $f_{neutral}$ is the neutral fraction of the single compound which lies between 0 and 1 and α takes a value of 1 for anionic chemicals (acids, e.g. CYA), and a value of -1 for cationic chemicals (bases, e.g. MEL).

The amount of complex was calculated assuming that if one can quantify the complex in moles, one mole of the complex was formed with one mole of MEL and one mole of CYA. Formation of the MEL-CYA complex was modelled with a first order rate, $k_{complex}$ ($mL^2.mol^{-1}.d^{-1}$) that multiplied the product of the molar concentrations of neutral single compounds (Eq. 2). At equimolar doses of both single compounds, the process therefore occurs at a velocity proportional to the square of single compound concentrations. No *in vitro* or *in vivo* data were available for the kinetics of MEL-CYA

complex formation and precipitation and , complex was assumed to form very rapidly compared to the length of time spent in the bladder by single compounds. $k_{complex}$ was fitted by testing values ranging from 10 to 10^5 and evaluating the quality of predictions of urinary or renal crystal concentrations.

$$dQ_{complex} = k_{complex} \times f_{MELneutral} \times C_{MELtissue} \times f_{CYAneutral} \times C_{CYAtissue} \quad \text{Eq. 2}$$

Crystal formation is assumed to occur as soon as the level of complex exceeds the limit of solubility (*S*) of the complex, around 31 µmol.L^{-1} in water (assuming a complex has one molecule of each of the single compounds) within pH 5-7 (Tolleson et al., 2009). Crystal formation is modelled as close to 0 when the concentration of dissolved complex $(Q_{complex}-Q_{crystal})/V_{kidney}$ is under the limit of solubility, *S* (µmol.mL^{-1}), and as first order kinetics with rate $k_{crystal}$ (d^{-1}) when the concentration of dissolved complex is over the limit of solubility (Eq 3). This is achieved with a Hill type equation with a very steep slope. The rate of precipitation, $k_{crystal}$, was set to 10^8 so that precipitation was very fast compared with complex formation.

$$dQ_{crystal} = k_{crystal} \times (Q_{complex} - Q_{crystal}) \quad \text{Eq. 3}$$

Scenarios of crystal formation

The nephron in freshwater teleost kidneys is a complex structure, similar to the structure observed in mammals (Hickman JR. and Trump, 1969). Physiological data on urine formation and kidney structure in fish, such as volume and flow of urine in the nephrons, and organic compound, ion, and water reabsorption, is too scarce to model the kidney structure and function precisely. We model the kidney as a well-mixed compartment from which MEL and CYA can be transferred to the bladder compartment with first order kinetics. Crystal formation was modelled according to two different scenarios: MEL-CYA crystals are either assumed to form (1) in the urine stored in the bladder or (2) in the kidney(Figure 1).

1. In scenario 1, there is no effect of the interaction on the internal kinetics of the single compounds as MEL-CYA crystals are assumed to form in urine stored in the bladder and the transfer rate from kidney to bladder is unchanged. Urinary pH was assumed to be neutral because freshwater fish excrete a large amount of dilute urine (Hickman JR. and Trump, 1969; Kleinow et al., 2008) even though a

large amount of urine produced at the kidney level is reabsorbed through the urinary bladder (Curtis and Wood, 1991). At pH 7, MEL is essentially unionized (pKa=5) and CYA is partly ionized (pKa=6.88).

2. In scenario 2, crystal formation is assumed to occur in the kidney tissue. Formation of the complex influences the kinetics of the single compounds by decreasing their concentrations in the kidney; this drags the single compounds from the rest of the organism to the kidney. The pH in the kidney tissue was assumed to be neutral. The crystals were assumed to be trapped in the kidney as a worst case scenario, because, although part of the crystals may be excreted in urine as in mammals (Stine et al., 2011), there is no data on which proportion of crystals may be excreted, or on any threshold on the rate of formation of the crystals above which the crystals may start to accumulate in the kidney. .

Evaluation of the predictions for mixtures

For both scenarios, predictions of MEL and CYA acid tissue concentrations were compared to the mixture toxicokinetic data available in the literature from four co-exposure studies (Table 1).

The predicted amount of MEL-CYA crystals in urine or in kidney was summarized by the maximal concentration (Cmax), the Area Under the Curve (AUC), and the concentration at the timepoint when the animals were sacrificed. In scenario 2, crystals accumulate in the kidney, therefore Cmax is equal to the concentration at the timepoint were animals were sacrificed. The relationship between crystal intensity observed on a 0-4 scale in kidney tissue by Reimschuessel et al. (2010) and Pacini et al. (2014) (Table 2) and the predicted amount of crystals was then studied using Spearman's correlation coefficient and ordered multinomial logistic regression models. Levels 1 and 2 were grouped together because these levels were rarely the most frequent outcome in a given condition (see Table 1 in SI). The significant descriptors were selected using a downwards stepwise variable selection on the Akaike Information Criterion (AIC) available in the MASS Package (Venables and Ripley, 2002) in R 3.3.1 (R Core Team, 2016) followed by a manual selection taking into account the correlation between the variables.

Results

Model calibration for toxicokinetics of single compounds

The parameter estimates are reported in Table 3 (sets of parameters producing maximum likelihood are reported in Table 3 SI). For CYA, as there was no data on the kinetics in liver, the liver to blood partition coefficient was set to 1.9, the estimate for MEL. For CYA, two slightly different sets of parameters were obtained, as two out of the six chains converged to a slightly different local optimum. The resulting difference in kinetics is negligible (Figure 1 in Supplementary Information).

Although there is a clear lack of data for CYA administered alone, the partition coefficients are of the same order of magnitude as those obtained for MEL, but with higher uncertainty on the estimates. The absorption and urinary excretion rates are one order of magnitude higher for CYA than for MEL.

MEL predictions were relatively accurate: 58% of predictions for mean points above the LOQ were within a 2-fold factor, and 96 % were within a 10-fold factor. MEL kinetics after single doses are faster in serum and muscle than predicted by our model (Figure 2B, C), which was adjusted to both single dose and repeated doses experiments. MEL kinetics in kidney were relatively accurate both following single doses (Figure 2A) and during repeated dosing (Figure 2D). In repeated dose exposure scenarios, muscle concentrations were underpredicted in study E (Figure 2D) and overpredicted in study F (Figure 2E). With repeated doses, kidney concentrations were slightly over-predicted and serum concentrations were slightly under-predicted in study E (Figure 2D).

Predicted CYA kinetics were faster than for MEL and the data only provided information in the depletion phase (Figure 3). 50% of predictions for mean points above the LOQ were within a 2-fold factor, and all were within a 10-fold factor.

Sensitivity to temperature

The sensitivity analysis of urinary excretion depending on temperature and cardiac output, urinary excretion rate, and oral absorption rate showed that, at 12°C, temperature had a large effect and it acted mostly by changing the absorption rate, and to a lesser extent the urinary excretion rate (See

section 3 in Supplementary Information). Urinary excretion was scarcely affected by cardiac output and the effect of temperature on cardiac output.

Crystal formation in urine (Scenario 1)

The relationship between the observed crystal intensity and the predicted kinetics of crystal formation has been described separately in the two datasets published by Reimschuessel et al. (2010) and Pacini et al. (2014). When the data was pooled, the model predicted high crystal intensity (levels 3 and 4) in the Pacini dataset whereas no crystal formation was predicted in the Reimschuessel dataset, whereas the same levels of crystal intensity were observed in both datasets. In the study by Pacini et al. (2014), higher exposure levels were necessary to elicit the same level as response as in Reimschuessel et al. (2010), which meant that the same model could not be used for both datasets. Furthermore, grouping levels 1 and 2 improved model accuracy (the proportion of correctly classified outcomes), which, given the variability within each condition, cannot exceed 76% and 73% in datasets by Reimschuessel et al. (2010) and Pacini et al. (2014) respectively.

Within the exposure scenarios investigated, when complex formation was fast, MEL concentration in urine was the limiting factor, because CYA is excreted rapidly but with much higher urinary concentrations (see urinary concentrations in the model without interactions, Figure 4A and B in main text and Figure 2 in SI). With low complex formation rate ($k_{complex}$ = 10), crystal formation occurred in urine only in sequential exposure scenarios starting with MEL or with daily co-exposure to 5 or 10 mg/kg/day (Figure 2 in SI, panels A2 MC, F 5 and F 10 and F 5). This result is in agreement with the crystal intensity data (Table 1 in SI) for cases under which no crystals were observed, but in lower dose or shorter exposure scenarios crystal formation was also observed. With a high complex formation rate ($k_{complex}$ = 10^5), crystal formation was overpredicted, as it was predicted to occur in all the exposure scenarios except in the sequential exposures with longest waiting period.

Accuracy was best when crystal intensity was predicted using the AUC of crystal concentration in urine and the final crystal concentration in urine with $k_{complex}$ equal to 10,000 $mL^2.mol^{-1}.d^{-1}$. Examples of kinetics are shown in Figure 5A and B; all exposure scenarios are shown in Figure 4 SI. Comparison of Figure 4A and B with Figure 5A and B illustrates to which extent MEL values were

decreased in urine when CYA was administered. With this value for $k_{complex}$, no crystal formation in urine was predicted to occur in exposure scenarios with the longest waiting period between exposure to the two single compounds (Figure 4 in SI, panels A2 20 MC and A2 20 CM). The number of outcomes correctly predicted was 74% and 65% in datasets by Reimschuessel et al. (2010) and Pacini et al. (2014) respectively (Figure 6). The maximal urinary crystal concentration predicted was around 300µg/mL for a 10-week exposure to 10 mg/kg/day.

In scenario 1, where intensity of MEL-CYA crystal formation is predicted based on the kinetics of both single compounds in urine, the tissue concentrations for which the mean values were above the LOQ were again better for MEL than for CYA. 74% of the predictions for MEL and 25% for CYA were within a 3-fold factor and 95% of the predictions for MEL and 71% for CYA were within a 10-fold factor (Figure 7**Error! Reference source not found.**). CYA tissue concentrations were mostly overpredicted (Figure 7D, F, and H), except in the kidney (Figure 7B) where a large amount of variability was observed, as noted by the authors of the study, with large amounts of MEL and CYA in some samples. As in studies with MEL administered as a single compound, MEL concentrations were overpredicted in study F, the 10-week experiment dataset by Pacini et al. (2013) (Figure 7I).

Crystal formation in kidney (Scenario 2)

In scenario 2, crystal formation kinetics can be different compared to scenario 1 because the MEL – CYA ratio is different: MEL concentrations are higher in the kidney tissue (see Figure 4C and D in main text and Figure 5 in SI). With low complex formation rate ($k_{complex}$ = 10), in scenario 2, crystal formation occurred in kidney after several days of exposure to 2.5, 5 or 10 mg/kg/day of MEL and CYA (Figure 6 in SI, panels F 2.5, F 5, and F 10). With a high complex formation rate ($k_{complex}$ = 10^5), crystal formation was overpredicted, as it was predicted to occur in all the exposure scenarios. Crystal formation noticeably impacted kidney concentrations when $k_{complex}$ was equal or greater than 1,000 $mL^2.mol^{-1}.d^{-1}$.

According to the rate of outcomes with good predictions using logistic regression, crystal intensity was best predicted for a $k_{complex}$ value equal to 10^3 $mL^2.mol^{-1}.d^{-1}$. Crystal formation in urine was predicted to occur in all simulations, but to a very low extent when MEL was administered 7 days

after CYA. The number of outcomes correctly predicted was 74% and 63% in datasets by Reimschuessel et al. (2010) and Pacini et al. (2014) respectively (Figure 6). Examples of kinetics in kidney are shown in Figure 5C and D in main text and Figure 7 in SI. Assuming all crystals were trapped in the kidney, the maximal renal crystal concentration predicted was almost 70 mg/mL after a 10-week exposure to 10 mg/kg/day.

In scenario 2, although crystal formation appeared extensive with a value of $k_{complex}$ of 10^3 $mL^2.mol^{-1}.d^{-1}$, it did not decrease kidney concentrations in MEL or CYA to a large extent. Unlike in scenario 1, where MEL was a limiting factor in complex formation in urine (Figure 5A and B), because kidneys are rapidly perfused, the decrease in free concentrations for the single compounds due to complex formation was rapidly compensated by blood flow: neither MEL nor CYA were limiting. In addition, MEL concentrations in the kidney were greater than CYA concentrations at equal dosages and the decrease in MEL levels occurred to a larger extent than the decrease in CYA levels (see levels in kidney in scenario 1, Figure 4C and D in main text and Figure 5 in SI). The kinetics of CYA when MEL is co-administered are shown in Figure 8 in SI). After a single dose of 20 mg/kg MEL and CYA, the MEL arterial blood concentration was predicted to decrease by 14% at Tmax, whereas the CYA arterial blood concentration only decreased by 1.7% at Tmax. With 14 daily doses of 2.5mg/kg/day, MEL and CYA concentrations in arterial blood at Tmax decrease by 12% and 5.7% respectively (9.7% for CYA at 14 days). The decrease in body concentrations resulting from crystal formation in the kidney improved the predictions for CYA in repeated dose exposure scenarios while having no effect on overall quality of prediction for MEL: 29% (compared to 25% in scenario 1) of CYA tissue concentration predictions for mean values above the LOQ were within a 3-fold factor and 79% (compared to 71% in scenario 1) were within a 10-fold factor.

Discussion

Availability of toxicokinetic experimental data for both single compound and mixtures together with toxicodynamic data in a single fish species in comparable experimental studies is extremely rare. The richness of toxicokinetic and toxicodynamic experimental data for the binary mixture of MEL and

CYA offered a unique opportunity to investigate the relationship between toxicokinetic and toxicodynamic processes using a rainbow trout PBTK model (Grech et al., 2019) and a toxicodynamic model.

Toxicokinetics of single compounds and of the binary mixture

The calibrated MEL PBTK model provided predictions which were a compromise between several sets of data collected at various temperatures, in different sized fish, with single and repeated dose studies. In the studies by Xue et al. (2011) and by Reimschuessel et al. (2009a), Stine et al. (2012), and Stine et al. (2013), MEL kinetics after a single dose were faster than predicted. Even when the model parameters were calibrated on the single dose studies, the kinetics following a single dose were not accurately modelled in all tissues (blood, poorly perfused tissues, and kidney). Adding a first order fecal excretion rate with an expected 10% fecal excretion at the end of the experiment did not improve the predictions. The estimates for liver:blood and other tissue:blood partition coefficients for MEL (1.9 and 0.57 respectively) were very close to the estimates obtained in swine by Buur et al. (2008) (1.47 and 0.71 respectively). The estimate of the kidney:blood partition coefficient was larger than the value estimated in swine (8.0 in rainbow trout vs. 2.8 in swine). High MEL levels in the kidney and slower depletion in the kidney compared with blood and muscle were observed in rainbow trout (Figure 2**Error! Reference source not found.**A). We tried introducing diffusion-limited rather than flow-limited kinetics for MEL and CYA in the kidney to delay the kinetics. This slightly improved the predictions for the depletion in the kidney by delaying the peak concentrations but failed to predict the slow decrease in concentrations over time. This did also not improve the predictions of the difference in time-course between kidney on the one side and blood and muscle in the other side (Figure 2B). These differences in kinetics may however be specific to the dataset by Reimschuessel et al. (2009a), Stine et al. (2012), and Stine et al. (2013): the accumulation in the repeated dose scenario (study E) is slightly overestimated in kidney and underestimated in blood and muscle (Figure 2D) which appears to be in contradiction with the slow residual depletion observed in the single dose study. Diffusion-limited kinetics in kidney, in scenario 2 of crystal formation, predicted concentrations of free MEL and CYA in kidney that were very low because the diffusion was not fast enough to compensate for

precipitation of MEL and CYA, and therefore, this alternative modelling failed to predict formation of any crystals in most exposure scenarios and was therefore not considered.

The CYA model was calibrated using toxicokinetic data from only one study where CYA was administered as a single dose. The higher estimated absorption and urinary excretion rates for CYA are consistent with the faster kinetics observed in rainbow trout and in rats (Jacob et al., 2012; Reimschuessel et al., 2009a; Stine et al., 2013; Stine et al., 2012; Xue et al., 2011). The high variability of CYA levels in kidneys was assumed to be due to variability in the extent of crystal formation between animals and within individual kidneys.

The high levels of MEL, and high level of variability, observed in kidneys in case of co-exposure to MEL and CYA (Figure 7) could be explained by the fact that crystals in the tissues may have been partly or completely dissolved during the sample preparation before determination of MEL concentrations. Some studies report dissolution of the crystals using a mixture of acetonitrile, water, and diethylamine (Puschner et al., 2007). Although crystals hardly dissolve naturally in tissues, when measuring crystal intensity, wet mount techniques had to be used because the formalin fixation used in histology rapidly dissolves MEL crystals and CYA crystals in kidney tissue (Reimschuessel et al., 2008; Stine et al., 2014). The studies used in this paper do not clearly state whether, or to what extent, the sample preparation before MEL or CYA measurement, which often involves acids and acetonitrile, dissolves the MEL-CYA crystals.

Only two absorption and excretion routes, oral uptake and urinary excretion, were included in rainbow trout PBTK model to MEL and CYA case study. Branchial excretion was not modelled here because MEL was unlikely to be excreted by the gills and although approximately half of CYA is ionized according to Eq. 1, its low logKow may limit branchial excretion. Branchial excretion could however contribute to the faster elimination observed compared to MEL. Data on CYA transport across gills would help check this assumption. This is of special importance in our model as it can affect predicted concentrations in kidney and urine and thereon the toxicodynamics of the mixture. Furthermore, our model does not include branchial excretion of ionized compounds as described by Erickson et al. (2006).

Impact of temperature on urinary excretion

Comparison of MEL kinetics following oral administration in channel catfish (*Ictalurus punctatus*) at 24.3°C and in rainbow trout at 12.5°C have shown faster kinetics in the warmer water fish (Reimschuessel et al., 2009a). In the model proposed by Grech et al. (2019), the effect of temperature on cardiac output is expected to have an indirect effect on branchial absorption and on branchial, renal, and biliary excretion. In our model, the temperature directly affects the oral absorption and urinary excretion rates and the sensitivity analysis showed that the amount excreted in the urine depended on the temperature mainly via the effect on absorption.

Differences in body temperature could partly explain differences in kinetics between mammals and fish. In rats, Sugita et al. (1991) report a half-life of 37.9 min in the upper intestine (k=26 d^{-1}). This value is approximately 100 times the rate estimated in rainbow trout at 16°C (Ku=0.19 d^{-1}). The difference in body temperature may only play a minor role as it explains a 5-fold difference according to Arrhenius' function.

Crystal formation model

The predicted intensity of crystal formation was similar for both scenarios. The final $k_{complex}$ that can be used for predicting crystal intensity is relatively high as it involves crystal formation in almost all tested exposure scenarios. However, if toxicodynamics are to be predicted without using the available data as a training set, by simply using the AUC of predicted crystal concentration in urine or in kidney, scenario 1 provides the best predictions, with $k_{complex}$=10. This is because in many conditions, absence of crystal formation was the most frequent outcome, therefore a low value of $k_{complex}$ correctly predicted more cases. Higher values of $k_{complex}$ imply higher predicted levels and discriminate the various levels of crystal intensity better.

Our pH-dependent renal crystal formation model (scenario 2) relies on simplistic assumptions on the kidney structure: the kidney is modelled as a homogeneous tissue separated from the urine in the bladder compartment by a barrier across which the single compounds are excreted. When present, the bladder size is variable across fish species. In rainbow trout, as in most teleosts, the bladder is actually

a widening of the duct between the kidney and the urogenital orifice (Curtis and Wood, 1991). Our model could be adjusted to other species by adjusting the length of time between bursts of urine, but scenario 1 does rely on the presence of a bladder. The crystal formation model could also be extrapolated to mammals, in particular as the nephron structure in mammals bears some resemblance with the structure in teleost fish (Hickman JR. and Trump, 1969) and thereon allow integration of data on urinary MEL-CYA crystals as collected in swine (Stine et al., 2011). Adjustments must be made, however, because urine in mammals is more concentrated, has an important role in nitrogenous waste excretion rather than osmotic regulation, and can have a variable pH.

Our crystal formation model presents several limitations. The solubility of MEL-CYA was assumed to be the same within the kidney tissue as observed *in vitro* in a cell-free environment. pH was assumed to be neutral and constant in kidney tissue and in urine. In mammals, urine acidifies in the first part of the proximal tubules, and then reaches a more neutral pH in the distal tubules (Gottschalk et al., 1960; Koeppen and Steinmetz, 1983). In teleost freshwater fish, pH and levels of the various compounds excreted and optionally reabsorbed may also vary along the proximal tubule as organic acids, water, and monovalent ions are gradually reabsorbed (Hickman JR. and Trump, 1969). The pH along the tubules remains largely unknown even in mammals, as noted in swine by Stine et al. (2011). The time-scale for crystal formation is likely in seconds, therefore local conditions may cause very localized crystal formation. pH could be modelled as being time-variant, or simply as being non-neutral. This would change the reaction kinetics as complex formation depends on the concentrations of the neutral forms, not the total concentrations. In our model, the neutral/ionized equilibrium was assumed to be instantaneous, therefore the reaction would never be limited by the concentration in neutral forms of MEL and CYA, but rather in case of fast complex formation, by the total concentration of either MEL or CYA.

Small crystals may be excreted via urine as in swine (Stine et al., 2011) but there was no data available on presence of crystals in fish urine. At some point, crystals may start aggregating in tubules and obstructing them as during kidney stone formation (Khan, 2017): intrarenal obstruction was appeared to play a significant role in renal failure observed in cats after co-exposure to MEL and CYA

(Puschner et al., 2007) and can be seen lined up in renal tubules in cat, fish, pig and rat (Puschner and Reimschuessel, 2011). Furthermore, the diameter of the spherulite and tubular structures observed by Reimschuessel et al. (2009a) in rainbow trout were of the same order of magnitude, 10 to 30 µm, as the inner diameter of the various nephron segments in skate fish (*Raja erinacea*), a marine elasmobranch, reported by Lacy and Reale (1985). In this species, the inner diameter varies along the nephron: the succession of bottlenecks and wider sections could facilitate obstruction by crystals, however, comparisons with nephrons from other vertebrates are difficult and tedious (Lacy and Reale, 1985). In freshwater trout, *Salmo aguabonita*, *S. gairdneri*, *S. trutta*, and *Salvelinus fontinalis*, the inner and outer tubular diameter was reported to decrease in the distal section compared to the proximal tubule and intermediate segment (Anderson and Loewen, 1975).

In scenario 2, the default assumption was that all crystals formed in the kidney tissue remained there. This resulted in large concentrations of MEL-CYA crystals in kidney tissue, which were approximately 10-fold the melamine concentration in short term exposure scenarios and which reached almost 70 mg/mL in 10-week exposures to 10 mg/kg/day. This value is 50-fold larger than the concentrations measured in kidneys of cat suffering from renal failure 48 hours after exposure to MEL and CYA (Puschner et al., 2007). Several modelling alternatives were available. For example, a fixed proportion of the crystals formed at a given timepoint could have been excreted: renal concentrations may then have been more realistic and this hypothesis would not have any effect on as the relationship between the predicted and observed crystal intensity, as the observed crystal intensity is unitless. More complex modeling alternatives included modelling excretion of MEL-CYA crystals with a first-order rate, or defining threshold on the rate of MEL-CYA crystals formation above which the crystals may start to accumulate in the kidney

Added values and limitations of the TK-TD mixture model

When MEL and CYA models were used without the toxicodynamic interaction, or with scenario 1 where no effect on single compound kinetics was expected, predictions for MEL concentrations in co-exposure studies were approximately as accurate as in the single compound studies. The CYA kinetics predictions in co-exposure studies were over-predicted. This could be due to a mixture effect (MEL-

CYA complex formation) or to poor extrapolation from single doses to repeated doses by the model. However, according to the studies by Reimschuessel et al. (2009a) and Stine et al. (2012), which were the only ones to report kinetics of CYA administered alone and combined with MEL, CYA muscle and serum concentrations were lower in case of co-exposure. Given the experimental setup was the same, this suggests that mixture effects may be a more likely cause of the decrease in CYA concentrations in muscle and serum.

The mixture effects on single compound concentrations observed in some studies, in particular delayed disposition of MEL and/or CYA (Reimschuessel et al., 2009a; Xue et al., 2011) and a decrease in CYA concentrations in muscle and serum observed by Reimschuessel et al. (2009a) and Stine et al. (2012), were however still not well predicted in scenario 2. Indeed, modelling crystal formation in the kidney tissue modified mainly the predictions of MEL toxicokinetics in case of single doses by decreasing the observed concentrations, without however resulting in a decrease in goodness-of-fit of the co-exposure data. The predicted decrease in CYA concentrations did improve the goodness-of-fit in repeated dose exposures – not in single dose exposure scenarios -, but since the CYA model was not calibrated on this type of data, the lack of fit in the co-exposure studies could be due to either mixture effects or to calibration of the single compound model on a small set of data. The mixture effects in scenarios with simultaneous exposure (part of the data by Reimschuessel et al. (2010) and the entire data produced by Pacini et al. (2014)) may actually be attributed to a larger extent to the route of exposure (feed vs. gavage) and timing (consecutive vs. staggered gavage) (Sprando et al., 2012). A decrease in bioavailability in case of co-exposure in feed, and, to a lesser extent, in case of simultaneous or immediately consecutive gavage could explain that the relationship between observed crystal intensity and predicted internal kinetics had to be analyzed separately depending on whether MEL and CYA were administered in feed or in gelatin capsules. Some authors suggested that MEL and CYA precipitate in the gastrointestinal tract, thus decreasing bioavailability (Pang et al., 2013; Reimschuessel et al., 2008). In the dataset by Reimschuessel et al. (2010), a combination of MEL and CYA was administered in gelatin capsules embedded in gelatin feed nuggets either in one capsule or with at least a one-day delay. According to the results obtained in rats by

Sprando et al. (2012), crystal intensity was expected to be overpredicted in simultaneous exposure and underpredicted in sequential exposure, but this was not observed. In studies where an impact was observed, the effect was mainly delayed deposition, excretion, and tissue accumulation. This effect could only be achieved by assuming that crystals form in various organs and slowly dissolve: tissue accumulation would then be observed if crystals that form in tissues are dissolved during sample preparation prior to single compound measurement. However, at the dose levels described here crystals are rarely observed in organs other than the kidney, unlike at higher doses, as in catfish by Pirarat et al. (2012) at 125 or 500 mg/kg of both compounds or by Reimschuessel et al. (2008) at 400 mg/kg doses of both compounds. Finally, in our PBTK model, the first-order renal excretion is invariant whatever the exposure conditions. In the highest exposure scenarios, where many fish developed renal crystals, the renal function may have been impaired without there being immediate health issues, as fish can endure more extensive renal damage than most mammals as they excrete most of their nitrogenous waste across the gills (Nelson et al., 1999; Reimschuessel et al., 2008). Renal damage, such as epithelial cell vacuolization and necrosis (Reimschuessel et al., 1989), could modify excretion of endogenous or xenobiotic compounds via changes in excretion rates or blood flow; it could also disturb osmoregulation and therefore affect the physiological parameters of the PBTK model. The resulting physiological changes have not been quantified and this could be a shortcoming of our PBTK model.

In scenario 2, the interaction between MEL and CYA affects the kinetics of MEL more than those of CYA. CYA is absorbed and excreted faster than MEL so that the decrease in its kidney concentrations caused by crystal formation in kidney drags less CYA out than MEL from the rest of the body. The percentage decrease of single compounds caused by crystal formation in the gut would lead to the same percentage decrease in tissue concentrations for both compounds because, in our model, absorption and elimination kinetics are first order processes. The resulting percentage decrease in tissue concentrations would imply that crystal formation in urine occurs at higher exposure doses or latter than in scenario 1.

Globally, generation and integration of more data on toxicokinetics and toxicodynamics of MEL and CYA would support a better understanding of the physical processes studied. In this context, new *in vivo* data on the kinetics of CYA and absorption/excretion routes (in particular, urinary excretion), have to be produced to provide further insights on the mechanisms involved as well as measurements of the MEL-CYA complex in the kidney and biomarkers of renal toxicity.

Conclusions

Data for the binary mixture of MEL and CYA provided a unique example of application of a PBTK model to investigate mechanisms of interactions owing to the availability of both toxicokinetic and toxicodynamic data in one fish species. Modelling the kinetics of both compounds simultaneously provided good predictions of the intensity of crystal formation, and news insights on the interaction mechanisms, in particular in the case of sequential exposures. In this latter case, the model showed how the order of exposures and the delay between them both play a critical role in crystal formation. The interaction between MEL and CYA is unusual as it is a physico-chemical reaction between the compounds themselves. In contrast, metabolic interactions including enzyme inhibition or induction are more frequently encountered and could also be modelled in fish with our mixture PBTK model.

The interaction model we developed for MEL and CYA has a mechanistic basis but could be greatly improved with additional data on urine formation and urinary excretion of xenobiotics in fish. Additional data on kinetics of CYA and the ratio between branchial and urinary excretion would also help parameterize the PBTK model.

Acknowledgements

This work was supported by the European Food Safety Authority (EFSA) and the French Ministry of Ecology and Sustainable Development [Contract numbers: EFSA/SCER/2014/06 and Program 190, respectively]. The authors wish to thank the French association ANRT (Association Nationale de la Recherche et de la Technologie) and Analytica LASER for their contribution to the work funding. The authors wish to thank Rik Oldenkamp and Leonie Lautz, Radboud Universiteit, for fruitful discussions about modelling MEL kinetics.

Disclaimer

The views in this publication do not necessarily represent those of EFSA and are those of the authors only.

Conflict of Interest Statement

The authors have nothing to disclose.

References

Anderson, B.G., Loewen, R.D., 1975. Renal morphology of freshwater trout. The American Journal of Anatomy, 143(1): 93-114.

Baynes, R.E., Riviere, J.E., 2010. Risks associated with melamine and related triazine contamination of food. Emerging Health Threats Journal 3(e5).

Beaudouin, R., Dias, V., Bonzom, J.M., Pery, A., 2012. Individual-based model of Chironomus riparius population dynamics over several generations to explore adaptation following exposure to uranium-spiked sediments. Ecotoxicology, 21(4): 1225-1239.

Bertelsen, S.L., Hoffman, A.D., Gallinat, C.A., Elonen, C.M., Nichols, J.W., 1998. Evaluation of log K-ow and tissue lipid content as predictors of chemical partitioning to fish tissues. Environmental Toxicology and Chemistry, 17(8): 1447-1455.

Brand, L.M. et al., 2012. Effects of melamine in young broiler chicks. Poultry Science, 91(8): 2022-2029.

Brown, C.A. et al., 2007. Outbreaks of renal failure associated with melamine and cyanuric acid in dogs and cats in 2004 and 2007. Journal of Veterinary Diagnostic Investigation, 19(5): 525-531.

Buur, J.L., Baynes, R.E., Riviere, J.E., 2008. Estimating meat withdrawal times in pigs exposed to melamine contaminated feed using a physiologically based pharmacokinetic model. Regulatory Toxicology and Pharmacology, 51(3): 324-331.

Casu, A. et al., 1997. Fire-retardant mechanistic aspects of melamine cyanurate in polyamide copolymer. Polymer Degradation and Stability, 58(3): 297-302.

Consoer, D.M., Hoffman, A.D., Fitzsimmons, P.N., Kosian, P.A., Nichols, J.W., 2014. Toxicokinetics of perfluorooctanoate (PFOA) in rainbow trout (Oncorhynchus mykiss). Aquatic Toxicology, 156: 65-73.

Curtis, B.J., Wood, C.M., 1991. The function of the urinary bladder *in vivo* in the freshwater rainbow trout. Journal of Experimental Biology, 155: 567-583.

Dorne, J.L. et al., 2013. Recent advances in the risk assessment of melamine and cyanuric acid in animal feed. Toxicology and Applied Pharmacology, 270(3): 218-229.

Erickson, R.J., McKim, J.M., Lien, G.J., Hoffman, A.D., Batterman, S.L., 2006. Uptake and elimination of ionizable organic chemicals at fish gills: I. Model formulation, parameterization, and behavior. Environmental Toxicology and Chemistry, 25(6): 1512-1521.

FAO (Food and Agriculture Organization of the United Nations), 2017. World aquaculture production of fish, crustaceans, molluscs, etc., by principal species in 2015. In: Statistics, Y.o.F.a.A. (Editor).

Gerlowski, L.E., Jain, R.K., 1983. Physiologically Based Pharmacokinetic Modeling - Principles and Applications. Journal of Pharmaceutical Sciences, 72(10): 1103-1127.

Gingerich, W.H., Weber, L.J., Larson, R.E., 1977. Hepatic accumulation, metabolism and biliary excretion of sulfobromophthalein by rainbow trout (Salmo gairdneri). Comparative Biochemistry and Physiology Part C: Comparative Pharmacology, 58(2): 113-120.

Gossner, C.M.E. et al., 2009. The Melamine Incident: Implications for International Food and Feed Safety. Environmental Health Perspectives, 117(12): 1803-1808.

Gottschalk, C.W., Lassiter, W.E., Mylle, M., 1960. Localization of urine acidification in the mammalian kidney. The American journal of physiology, 198: 587-585.

Grech, A. et al., 2017. Toxicokinetic models and related tools in environmental risk assessment of chemicals. Science of the Total Environment, 578: 1-15.

Grech, A. et al., 2019. Generic physiologically-based toxicokinetic modelling for fish: Integration of environmental factors and species variability. Science of the Total Environment, 651: 516-531.

Hickman JR., C.P., Trump, B.F., 1969. The kidney. In: Hoar, W.S., Randall, D.J. (Eds.), Fish Physiology Volume 1: Excretion, Ionic Regulation, and Metabolism, pp. 91-239.

Jacob, C.C., Von Tungeln, L.S., Vanlandingham, M., Beland, F.A., da Costa, G.G., 2012. Pharmacokinetics of Melamine and Cyanuric Acid and Their Combinations in F344 Rats. Toxicological Sciences, 126(2): 317-324.

Jutzi, K., Cook, A.M., Hutter, R., 1982. The degradative pathway of the s-triazine melamine. The steps to ring cleavage. Biochem J, 208(3): 679-84.

Khan, S.R., 2017. Histological aspects of the "fixed-particle" model of stone-formation: animal studies. Urolithiasis, 45(1): 75-87.

Kleinow, K.M., Nichols, J.W., Hayton, W.L., McKim, J.M., Barron, M.G., 2008. Toxicokinetics in fishes. In: Hinton, D., Di Giulio, R. (Eds.), The Toxicology of Fishes.

Koeppen, B.M., Steinmetz, P.R., 1983. Basic mechanisms of urinary acidification. Med Clin North Am, 67(4): 753-70.

Kooijman, S., 2010. Notation of Dynamic Energy Budget theory for metabolic organisation. Cambridge University Press.

Lacy, E.R., Reale, E., 1985. The elasmobranch kidney. II. Sequence and structure of the nephrons. Anatomy and Embryology, 173(2): 163-186.

Liu, H.Y. et al., 2014. Tissue deposition and residue depletion in rainbow trout following continuous voluntary feeding with various levels of melamine or a blend of melamine and cyanuric acid. Comparative Biochemistry and Physiology C-Toxicology & Pharmacology, 166: 51-58.

Mast, R.W., Jeffcoat, A.R., Sadler, B.M., Kraska, R.C., Friedman, M.A., 1983. METABOLISM, DISPOSITION AND EXCRETION OF MELAMINE-C-14 IN MALE FISCHER-344 RATS. Food and Chemical Toxicology, 21(6): 807-810.

Miller, D.S., 1987. Aquatic models for the study of renal transport function and pollutant toxicity. Environ Health Perspect, 71: 59-68.

Nagel, R., Urich, K., 1980. Kinetic studies on the elimination of different substituted phenols by goldfish (Carassius auratus). Bulletin of Environmental Contamination and Toxicology, 24(1): 374-378.

Nelson, K., Jones, J., Jacobson, S., Reimschuessel, R., 1999. Elevated Blood Urea Nitrogen (BUN) Levels in Goldfish as an Indicator of Gill Dysfunction AU - Nelson, Keith. Journal of Aquatic Animal Health, 11(1): 52-60.

Nichols, J.W. et al., 1990. A physiologically based toxicokinetic model for the uptake and disposition of waterborne organic chemicals in fish. Toxicology and Applied Pharmacology, 106(3): 433-447.

Nichols, J.W., Schultz, I.R., Fitzsimmons, P.N., 2006. In vitro-in vivo extrapolation of quantitative hepatic biotransformation data for fish - I. A review of methods, and strategies for incorporating intrinsic clearance estimates into chemical kinetic models. Aquatic Toxicology, 78(1): 74-90.

Pacini, N. et al., 2014. Melamine–cyanurate complexes and oxidative stress markers in trout kidney following melamine and cyanuric acid long-term co-exposure and withdrawal. Fish Physiology and Biochemistry, 40(5): 1609-1619.

Pacini, N. et al., 2013. Antioxidant Responses and Renal Crystal Formation in Rainbow Trout Treated with Melamine Administered Individually or in Combination with Cyanuric Acid. Journal of Toxicology and Environmental Health-Part a-Current Issues, 76(8): 491-508.

Pang, J. et al., 2013. Toxicokinetic study of melamine in the presence and absence of cyanuric acid in rats. Journal of Applied Toxicology, 33(6): 444-450.

Pery, A.R.R. et al., 2014. A Physiologically Based Toxicokinetic Model for the Zebrafish Danio rerio. Environmental Science & Technology, 48(1): 781-790.

Phromkunthong, W., Choochuay, P., Kiron, V., Nuntapong, N., Boonyaratpalin, M., 2015. Pathophysiological changes associated with dietary melamine and cyanuric acid toxicity in red tilapia. Journal of Fish Diseases, 38(2): 161-173.

Pirarat, N. et al., 2012. The Pathological Effects of Melamine and Cyanuric Acid in the Diet of Walking Catfish (Clarius batrachus). Journal of Comparative Pathology, 147(2-3): 259-266.

Pritchard, J.B., Renfro, J.L., 1984. Interactions of xenobiotics with teleost renal function. Aquatic Toxicology, 2: 51-106.

Puschner, B., Poppenga, R.H., Lowenstine, L.J., Filigenzi, M.S., Pesavento, P.A., 2007. Assessment of melamine and cyanuric acid toxicity in cats. Journal of Veterinary Diagnostic Investigation, 19(6): 616-624.

Puschner, B., Reimschuessel, R., 2011. Toxicosis Caused by Melamine and Cyanuric Acid in Dogs and Cats: Uncovering the Mystery and Subsequent Global Implications. Clinics in Laboratory Medicine, 31(1): 181-199.

R Core Team, 2016. R: A Language and Environment for Statistical Computing. R Foundation for Statistical Computing.

Reimschuessel, R., Bennett, R.O., May, E.B., Lipksy, M.M., 1989. Renal histopathological changes in the goldfish (Carassius auratus) after sublethal exposure to hexachlorobutadiene. Aquatic Toxicology, 15(2): 169-180.

Reimschuessel, R. et al., 2009a. Residue depletion of melamine and cyanuric acid in catfish and rainbow trout following oral administration. Journal of Veterinary Pharmacology and Therapeutics, 33(2): 172-182.

Reimschuessel, R. et al., 2010. Renal crystal formation after combined or sequential oral administration of melamine and cyanuric acid. Food and Chemical Toxicology, 48(10): 2898-2906.

Reimschuessel, R. et al., 2008. Evaluation of the renal effects of experimental feeding of melamine and cyanuric acid to fish and pigs. American Journal of Veterinary Research, 69(9): 1217-1228.

Reimschuessel, R., Hattan, D.G., Gu, Y., 2009b. Background Paper on Toxicology of Melamine and Its Analogues, World Health Organization.

Schmidt, D.C., Weber, L.J., 1973. Metabolism and Biliary Excretion of Sulfobromophthalein by Rainbow Trout (Salmo gairdneri). Journal of the Fisheries Research Board of Canada, 30(9): 1301-1308.

Seffernick, J.L., Dodge, A.G., Sadowsky, M.J., Bumpus, J.A., Wackett, L.P., 2010. Bacterial Ammeline Metabolism via Guanine Deaminase. Journal of Bacteriology, 192(4): 1106-1112.

Seto, C.T., Whitesides, G.M., 1990. Self-assembly based on the cyanuric acid-melamine lattice. Journal of the American Chemical Society, 112(17): 6409-6411.

Skinner, C.G., Thomas, J.D., Osterloh, J.D., 2010. Melamine Toxicity. Journal of Medical Toxicology, 6: 50-55.

Sprando, R.L. et al., 2012. Timing and route of exposure affects crystal formation in melamine and cyanuric exposed male and female rats: Gavage vs. feeding. Food and Chemical Toxicology, 50(12): 4389-4397.

Stine, C.B. et al., 2013. Depletion of melamine and cyanuric acid in kidney of catfish Ictalurus punctatus and trout Oncorhynchus mykiss. Journal of Veterinary Pharmacology and Therapeutics, 36(6): 617-620.

Stine, C.B. et al., 2012. Depletion of melamine and cyanuric acid in serum from catfish Ictalurus punctatus and rainbow trout Onchorhynchus mykiss. Food and Chemical Toxicology, 50(10): 3426-3432.

Stine, C.B. et al., 2011. A No Observable Adverse Effects Level (NOAEL) for pigs fed melamine and cyanuric acid. Regulatory Toxicology and Pharmacology, 60(3): 363-372.

Stine, C.B. et al., 2014. Reproductive toxicity in rats with crystal nephropathy following high doses of oral melamine or cyanuric acid. Food and Chemical Toxicology, 68: 142-153.

Sugita, T., Ishiwata, H., Maekawa, A., 1991. INTESTINAL-ABSORPTION AND URINARY-EXCRETION OF MELAMINE IN MALE WISTAR RATS. Journal of the Food Hygienic Society of Japan, 32(5): 439-443.

Thomas, R.E., Rice, S.D., 1982. Metabolism and clearance of phenolic and mono-, di- and polynuclear aromatic hydrocarbons by Dolly Varden char. Physiological Mechanisms of Marine Polluant Toxicity 425-448.

Tolleson, W.H., 2010. Renal toxicity of pet foods contaminated with melamine and related compounds. In: Al-Taher, F., Jackson, L., DeVries, J.W. (Eds.), Intentional and Unintentional Contaminants in Food and Feed. American Chemical Society.

Tolleson, W.H., Diachenko, G.W., Folmer, D., Doell, D., Heller, D., 2009. Background Paper on the Chemistry of Melamine Alone and in Combination with Related Compounds.

Venables, W.N., Ripley, B.D., 2002. Modern Applied Statistics with S. Springer, New York.

Wackett, L.P., Sadowsky, M.J., Martinez, B., Shapir, N., 2002. Biodegradation of atrazine and related s-triazine compounds: from enzymes to field studies. Applied Microbiology and Biotechnology, 58(1): 39-45.

Wang, W., Chen, H., Yu, B., Mao, X.B., Chen, D.W., 2014. Tissue deposition and residue depletion of melamine in fattening pigs following oral administration. Food Additives and Contaminants Part a-Chemistry Analysis Control Exposure & Risk Assessment, 31(1): 7-14.

Xing, H.J. et al., 2014. Effects of atrazine and chlorpyrifos on cytochrome P450 in common carp liver. Chemosphere, 104: 244-250.

Xue, M. et al., 2011. Plasma pharmacokinetics of melamine and a blend of melamine and cyanuric acid in rainbow trout (Oncorhynchus mykiss). Regulatory Toxicology and Pharmacology, 61(1): 93-97.

Zapletal, D., Strakova, E., Novak, P., Suchy, P., 2016. Broiler chickens exposed to melamine and cyanuric acid-contaminated diets. Hum Exp Toxicol, 35(7): 760-6.

Tables and figures

Table 1: Summary on toxicokinetic data for melamine and cyanuric acid in rainbow trout

Study reference	Dose MEL (mg/kg/day)	Dose CYA (mg/kg/day)	Single / repeated	Mode of administration	Average fish weight at start of experiment	Temperature	Food level per day (% BW)	Tissues
A1 Reimschuessel et al. (2009a) (a) Stine et al. (2013) (b) Stine et al. (2012) (c)	20 20	 20 20	single dose	bolus, in capsule, by gavage	408 g	12.5 °C	1-4 %	muscle (fillet)[a], kidney[b], serum[c]
D Xue et al. (2011) (d)	20 5	 1.67	single dose	in diet, fed only once	107 g	16 °C	1 %	plasma[d]
E Liu et al. (2014) (e)	20 5	 1.67	42-day	in diet, fed twice a day	124 g	15 °C	1 %	plasma, liver, kidney, muscle, gills[e]
F Pacini et al. (2013) (f)	2.5, 5, 10 2.5, 5, 10	 2.5, 5, 10	56-day	in diet	351 g	10 °C	1 %	muscle[f]

Table 2 : Summary of data on MEL-CYA crystal formation in rainbow trout

Study reference	Dose MEL (mg/kg/day)	Dose CYA (mg/kg/day)	Exposure scenario	Mode of administration	Average fish weight at start of experiment	Temperature	Food level per day (% BW)
A2 Reimschuessel et al. (2010)[g]	10	10	1 d	Capsule, by gavage	553.1 ± 190.4 g	12.5°C in A1	1-4 %
	5	5	1 d, 4 d				
	2.5	2.5	1 d, 4 d, 14 d				
	1	1	14 d				
	0.5	0.5	14 d				
	20	20	MEL then CYA at 1, 3, 7, 14, 21 d intervals				
	20	20	CYA then MEL at 1, 3, 7 d intervals				
F[f] Pacini et al. (2014)	2.5, 5, 10	2.5, 5, 10	every week for 10 weeks	in diet	350.7 g	10 °C	1 %

Table 3 : Compound-specific parameter estimates

Parameter	Estimate (mean ± sd)	
	Melamine	Cyanuric Acid (chain4)
Absorption rate (Ku)	0.19±0.0043 d^{-1}	1.1±0.045 d^{-1}
Urinary excretion rate (Ke_urine)	10±0.71 d^{-1}	236±20 d^{-1}
Liver:Blood partition coefficient	1.9± 0.22	-
Kidney:Blood partition coefficient	8.0±0.66	2.1±0.41
Poorly perfused tissue:Blood partition coefficient	0.57±0.038	0.18±0.032

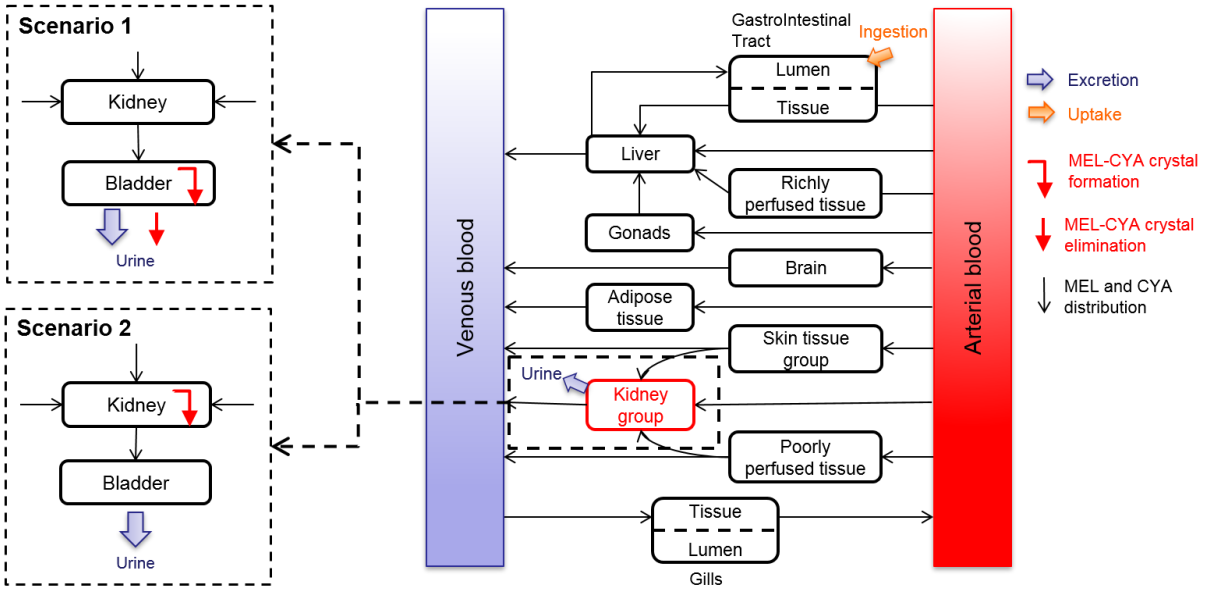

Figure 1: Schematic description of the PBTK model for rainbow trout (Grech et al., 2019) adapted to MEL and CYA, with two scenarios of crystal formation.

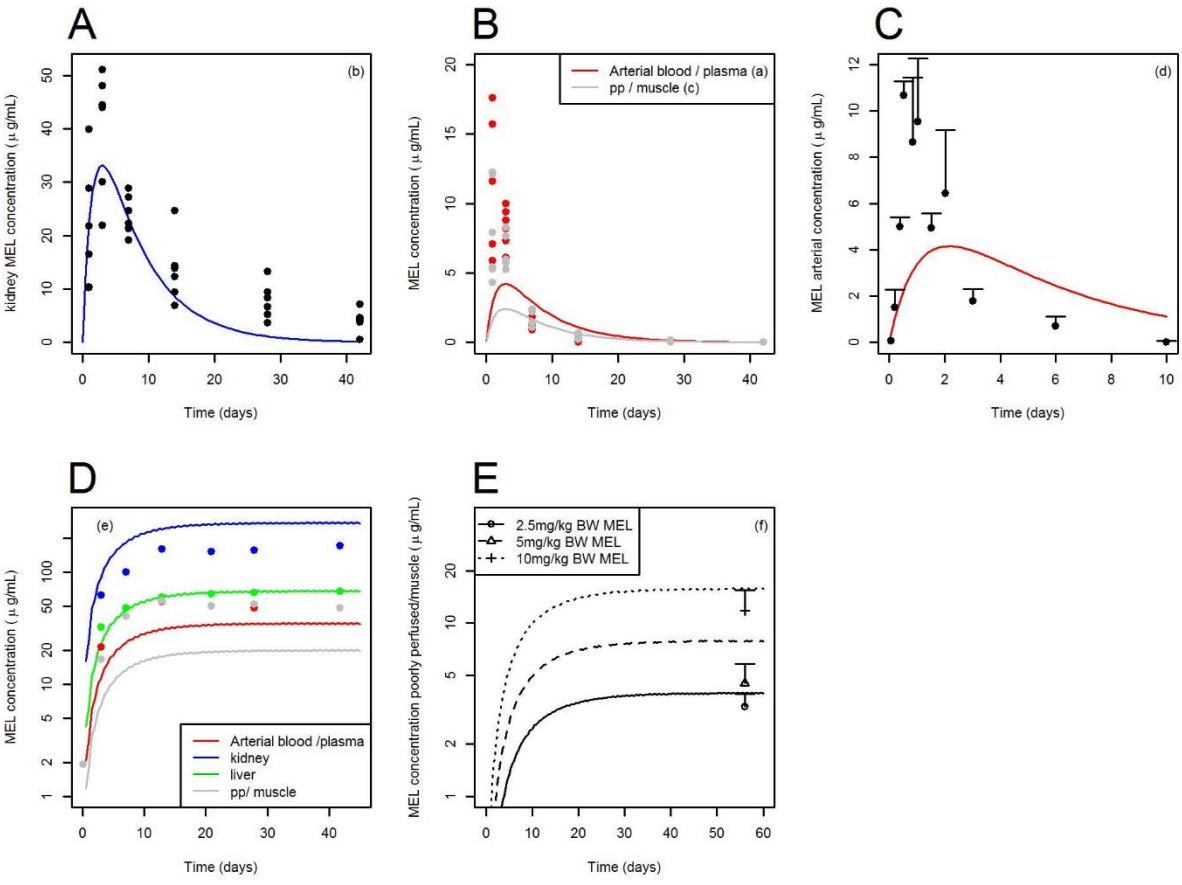

Figure 2 : Predicted and observed melamine concentrations in A) kidney, with data from Stine et al. (2013) B) blood and poorly perfused tissues, with data in serum from Reimschuessel et al. (2009a) and in muscle from Stine et al. (2012), C) blood with data in plasma from Xue et al. (2011), D) kidney, blood, poorly perfused tissues, and liver with data from Liu et al. (2014), E) poorly perfused tissues, with data in muscle from Pacini et al. (2013). The letters in brackets refer to the data source in Table 1.

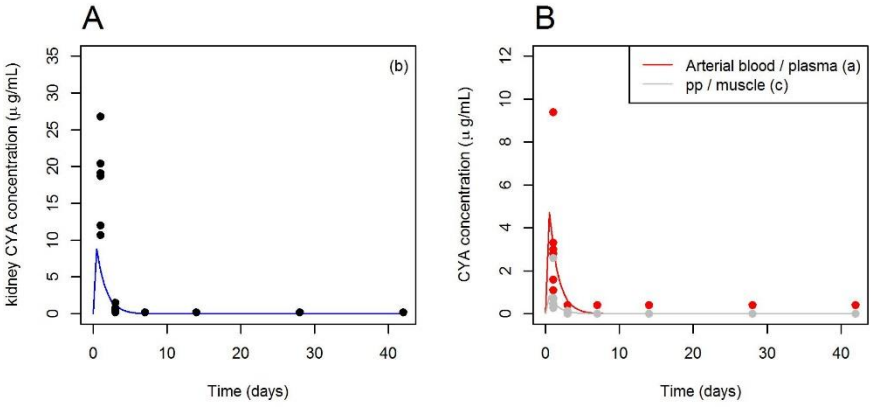

Figure 3: Predicted and observed cyanuric acid concentrations in A) kidney, B) blood (data in serum) and poorly perfused tissues (data in muscle). The letters in brackets refer to the data source in Table 1.

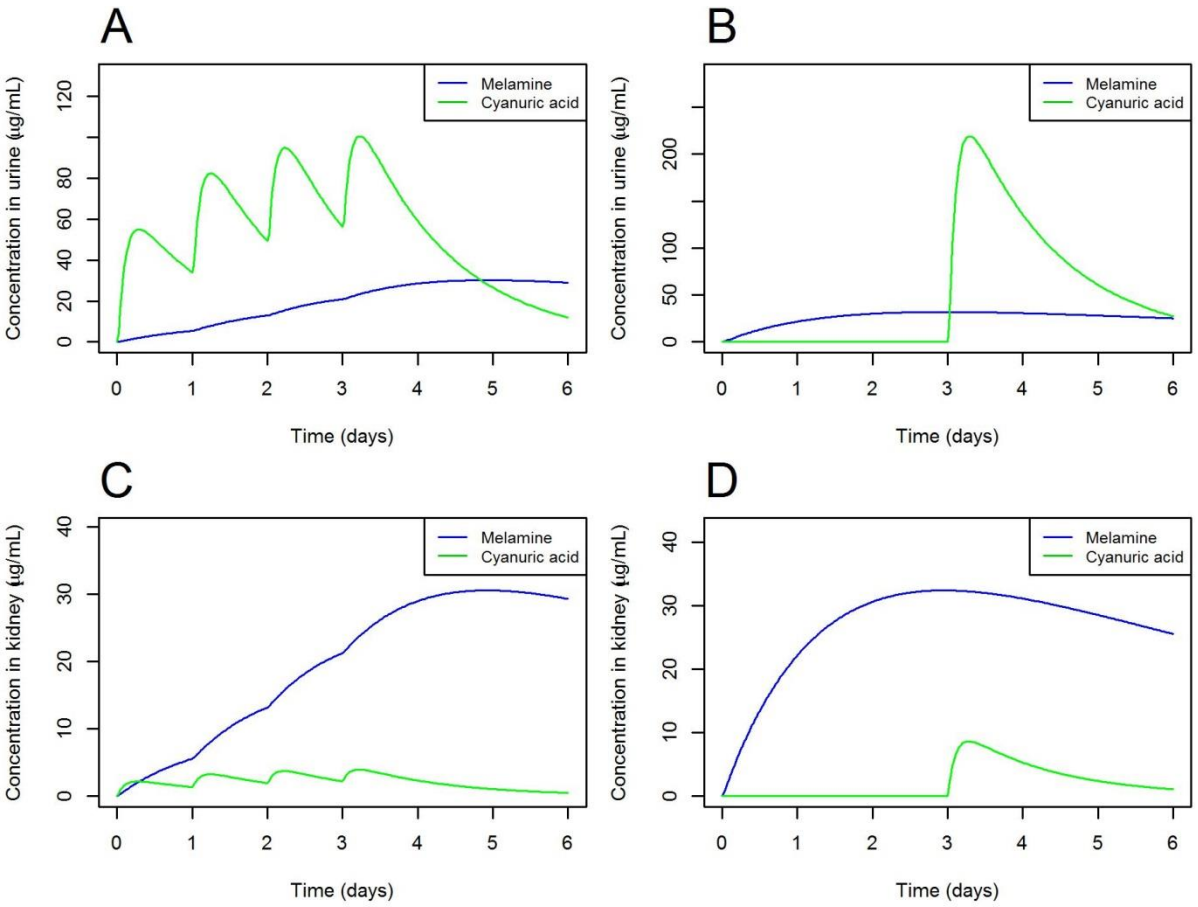

Figure 4: Predicted single compound concentration without complex formation in urine (A and B) and in kidney (C and D). A) and C) 3 daily doses of 5mg/kg/day melamine and cyanuric acid; B) and D)20mg/kg melamine followed by 20mg/kg cyanuric acid 3 days later;).

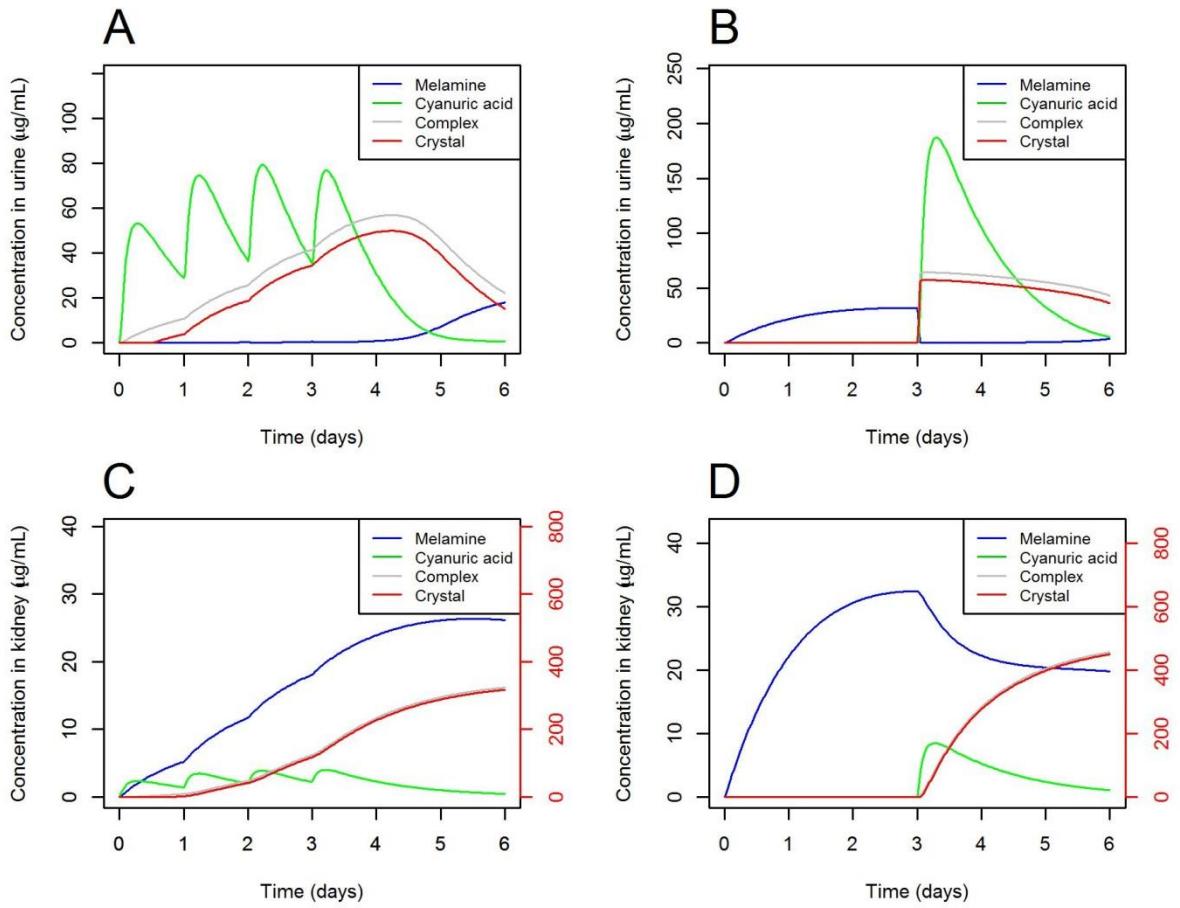

Figure 5: Predicted single compound and crystal concentration in urine with scenario 1 with $k_{complex}$=10,000 (A and B) and in kidney with scenario 2 and $k_{complex}$=1,000 (C and D). A) and C) 3 daily doses of 5mg/kg/day melamine and cyanuric acid; B) and D)20mg/kg melamine followed by 20mg/kg cyanuric acid 3 days later;). The red axes represent concentration of complex and crystals (µg/mL).

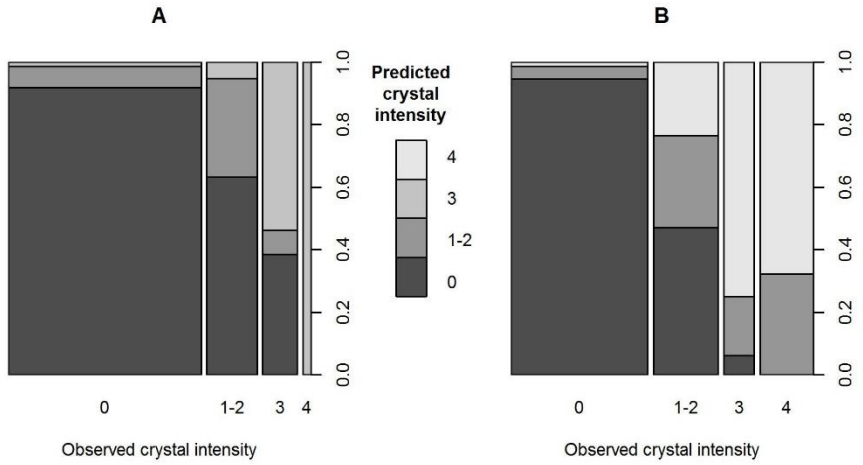

Figure 6: Spine plot of observed and predicted crystal intensity for the studies by (A) Reimschuessel et al. (2010) after 1, 4, 14, or 28 daily doses of MEL and CYA in combination, and after sequential exposures to MEL and CYA with several waiting periods between doses and (B) (Pacini et al. (2014)) every week over 10-week exposures. For observed

crystal intensity 0, good predictions are represented in dark grey. For observed crystal intensity 4, good predictions are represented in light grey. Predictions are obtained with the amount of crystals formed in urine in scenario 1.

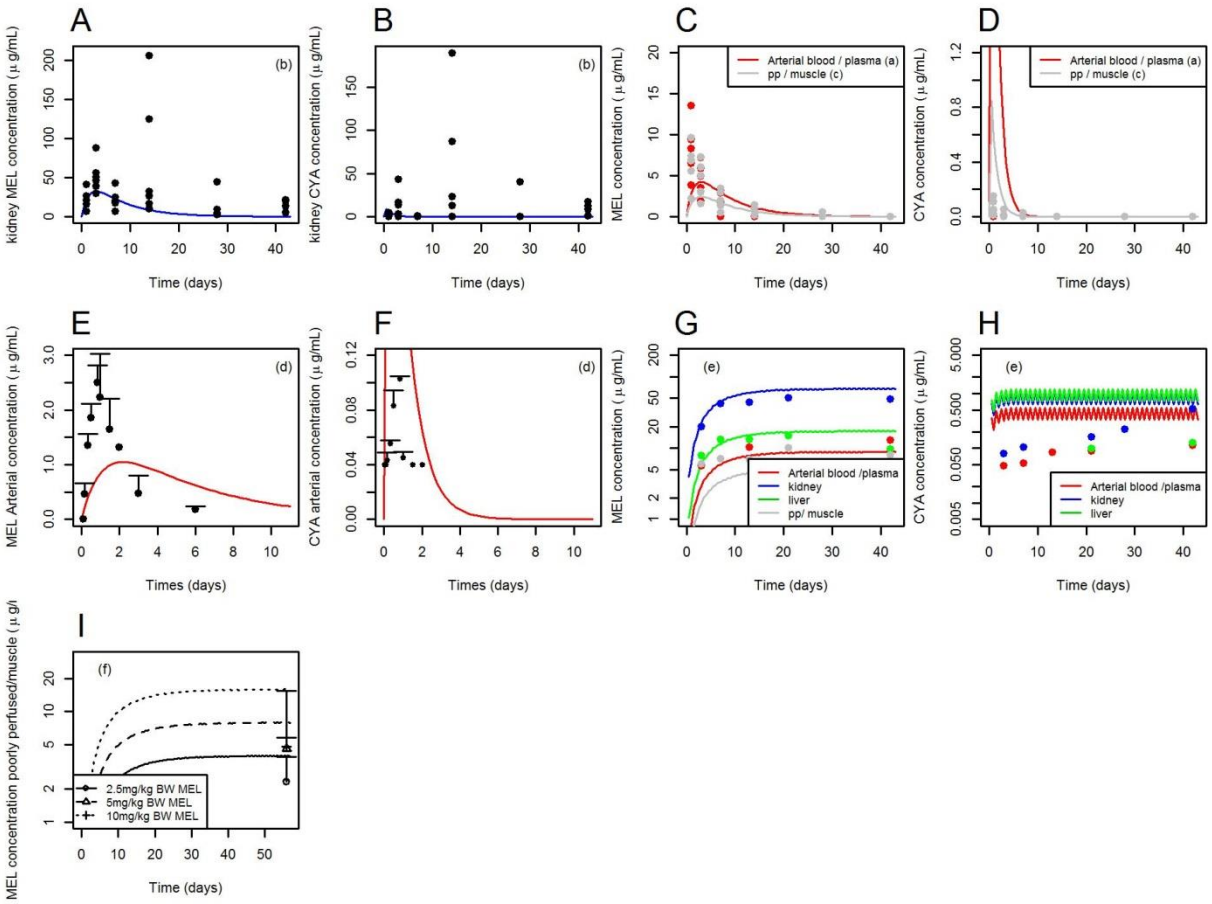

Figure 7: Predicted and observed melamine (A, C, E, G, I) and cyanuric acid (B, D, F, H) concentrations following MEL and CYA co-administration and without interactions between MEL and CYA in A), B) kidney after exposure to 20 mg/kg MEL and CYA; C), D) blood (data in serum), poorly perfused tissues (data in muscle) after exposure to 20 mg/kg MEL and CYA; E), F) blood (data in plasma) after exposure to 5 mg/kg MEL and 1.67 mg/kg CYA; G), H) blood, liver, kidney, and muscle during repeated exposure to 5 mg/kg MEL and 1.67 mg/kg CYA. The letters in brackets refer to the data source in Table 1.

Highlights

- Formation of melamine cyanurate crystals was modelled as a first order process
- A toxicodynamic component was added to a toxicokinetic model in fish
- Intensity in case of sequential exposure depends on single compound toxicokinetics
- Lack of data on chemical-specific excretion in fish hinders model development